Asociación Argentina de Mecánica Computacional

Mecánica Computacional Vol XXXI, págs. 2575-2591 (artículo completo)
Alberto Cardona, Paul H. Kohan, Ricardo D. Quinteros, Mario A. Storti (Eds.)
Salta, Argentina, 13-16 Noviembre 2012

BOUNDARY AND EIGENVALUE PROBLEMS FOR ANISOTROPIC PLATES WITH SEVERAL INTERNAL LINE HINGES

Javier L. Raffo[a], **Ricardo O. Grossi**[b]

[a]*Grupo de Mecánica Computacional, Universidad Tecnológica Nacional Facultad Regional Delta, San Martin 1171, 2804 Campana, Argentina, jraffo@frd.utn.edu.ar, http://www.frd.utn.edu.ar/grupo-de-mecanica-computacional*

[b]*INIQUI - ICMASA - Facultad de Ingeniería - Universidad Nacional de Salta, Av. Bolivia 5150, 4400 Salta, Argentina, grossiro@unsa.edu.ar, http://www.unsa.edu.ar/iniqui/*

Keywords: Anisotropic plates, internal line hinges, vibrations.

Abstract. The present paper deals with the free transverse vibration of a tapered anisotropic plate with several arbitrarily located internal line hinges and non-smooth boundary, elastically restrained against rotation and translation.

The equations of motion and its associated boundary and transition conditions are rigorously derived using Hamilton's principle. The governing eigenvalue problem is solved employing a combination of the Ritz method and the Lagrange multipliers method.

The deflections of the plate and the Lagrange multipliers are approximated by polynomials as coordinate functions. The developed algorithm allows obtaining approximate solutions for plates with different geometries and boundary conditions, including edges and line hinges elastically restrained.

In order to obtain an indication of the accuracy of the developed mathematical model, some cases available in the literature are considered. New results are presented for different boundary conditions and restraint conditions in the internal line hinges.

1 INTRODUCTION

Substantial literature has been devoted to the formulation, by means of the calculus of variations of boundary value problems of mathematical physics (Courant and Hilbert, 1953; Guelfand and Fomin, 1963; Kantorovich and Krylov, 1964; Mikhlin, 1964; Sagan, 1969; Bliss, 1971; Weinstock, 1974; Ewing, 1985; Leitmann, 1986; Brechtken-Manderscheid, 1991; Blanchard and Brüning, 1992; Giaquinta and Hildebrandt, 1996; Troutman, 1996). Several books treated the study of isotropic and anisotropic plates including the determination of static, buckling and vibrations characteristics (Dym and Shames, 1973; Szilard, 1974; Timoshenko and Krieger, 1959; Lekhnitskii, 1968; Whitney, 1987; Reddy, 1997; Jones, 1999; Grossi, 2010). It is not the intention to review the literature consequently; only some of the published papers related to the present work will be cited. A great number of articles treated the dynamical behavior of plates with complicating effects such as: elastically restrained boundaries, presence of elastically or rigidly connected masses, variable thickness, anisotropic material, points and lines supports, presence of holes, etc. A review of the literature has shown that there is only a limited amount of information for the vibration of plates with line hinges. A line hinge in a plate can be used to facilitate folding of gates and to simulate a through crack along the interior of the plate, among other applications. Wang et al. (2001) studied the vibration of plates with an internal line hinge by using the Ritz method. Gupta and Reddy (2002) presented the exact buckling loads and vibration frequencies of orthotropic rectangular plates with an internal line hinge by employing an analytical method which applies the Levy solution and the domain decomposition technique. Xiang and Reddy (2003) provided the first-known solutions based on the first order shear deformation theory for vibration of rectangular plates with an internal line hinge. The Lévy method and the state-space technique were employed to solve the vibration problem. Huang et al. (2009) developed a discrete method for analyzing the free vibration problem of thin and moderately thick rectangular plates with a line hinge and various classical boundary conditions. Quintana and Grossi (2012) dealt with the study of free transverse vibrations of rectangular plates with an internal line hinge and elastically restrained boundaries. The governing eigenvalue equation was solved employing a combination of the Ritz method and the Lagrange multiplier method. All of these studies have considered rectangular plates with only one free internal line hinge. However, there is no previous study for the vibration of anisotropic plates with generally restrained piecewise-smooth boundaries and with several internal lines hinges elastically restrained against rotation and translation.

Engineers and applied mathematicians increasingly used the techniques of calculus of variations to solve a large number of problems and in this discipline the "operator" has been assigned special properties and handled using heuristic procedures. Commonly the domain of definition of a functional and the space of admissible directions of the variation of this functional are not clearly stated, thus most of the analytical manipulations are confusing and not mathematically precise. Grossi (2012) formulated an analytical model for the dynamic behaviour of anisotropic plates, with an arbitrarily located internal line hinge with elastics supports and piecewise-smooth boundaries elastically restrained against rotation and translation among other complicating effects. By introducing an adequate change of variables, the energies which correspond to the different elastic restraints, are handled in a rigorous framework. In the same manner in the present paper the application of the Hamilton's principle is used for the derivation of equations of motion and its associated boundary and transition conditions for anisotropic plates with several arbitrarily located internal lines hinges with elastics supports and piecewise smooth boundaries elastically restrained against rotation and translation. Also a methodology based on a combination of the Ritz method and the Lagrange multipliers method with polynomials as coordinate functions is used to investigate the natural frequencies and mode shapes. To demonstrate the validity and efficiency of the proposed algorithm, results of a convergence study are included, several numerical examples not previously treated are presented and some particular cases are compared with results presented by other authors. Tables and figures are given for frequencies, and two-dimensional plots for mode shapes are included.

The complicating effects such as: elastically restrained piecewise smooth boundary, variable thickness, anisotropic material and several internal lines hinges lead to complicated analytical expressions and tedious algebraic manipulations. For this reason, in this paper a new analytical manipulation based on a condensed notation is used. The compact analytical expressions substantially lower the analytical effort and the amount of information.

2 THE ENERGY FUNCTIONAL

Let us consider an anisotropic plate that in the equilibrium position covers the two-dimensional domain G, with piecewise smooth boundary ∂G elastically restrained against rotation and translation. The plate has $N-1$ intermediate lines hinges elastically restrained against rotation and translation, as it is shown in Figure 1 In order to analyze the transverse displacements of the system under study we suppose that the vertical position of the plate at any time t, is described by the function $w=w(x,t)$, where $x=(x_1,x_2)\in\bar{G}$, $\bar{G}=G\cup\partial G$ and that the domain G is divided by the lines $\Gamma^{(c_k)}, k=1,2,\ldots,N-1$, into N parts $G^{(k)}$ with boundaries $\partial G^{(k)}$, (see Figure 1). Different rigidities $D_{lm}^{(k)}(x)$ and mass density $(\rho h)^{(k)}(x)=\rho^{(k)}(x)h^{(k)}(x)$ of the anisotropic material correspond to each sub-domain $G^{(k)}$. The extreme points a_k and b_k of the lines $\Gamma^{(c_k)}$ divide the boundary curve ∂G such that (see Figure 2):

$$\partial G=\Gamma^{(1)}\cup\Gamma^{(2)}\ldots\cup\Gamma^{(N)} \tag{1}$$

and

$$\Gamma^{(k)}=\partial G^{(k)}-\Gamma^{(c_{k-1})}-\Gamma^{(c_k)},\ k=1,2,\ldots,N \tag{2}$$

where $\Gamma^{(c_0)}=\phi$, $\Gamma^{(c_N)}=\phi$ and

$$\Gamma^{(k)}=\Gamma^{(k,1)}\cup\Gamma^{(k,2)}, k=2,3,\ldots,N-1. \tag{3}$$

Let us assume that the boundary curve ∂G is described by a smooth path γ in $\mathbb{R}^2$ defined in the compact interval $\left[0,l\right]$, where $l=l(\partial G)$ is the length of the path γ. The image of $\left[0,l\right]$ under γ (the graph of γ) is the boundary curve ∂G and will be denoted by $im(\gamma)$.

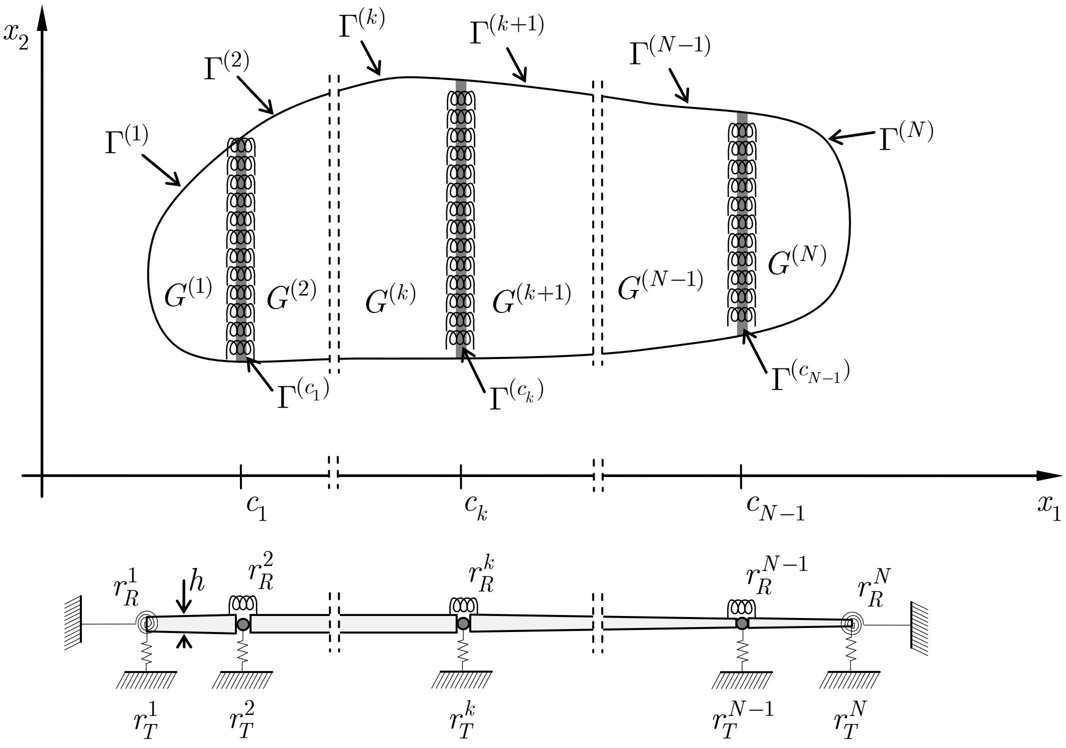

Figure 1: Mechanical system under study.

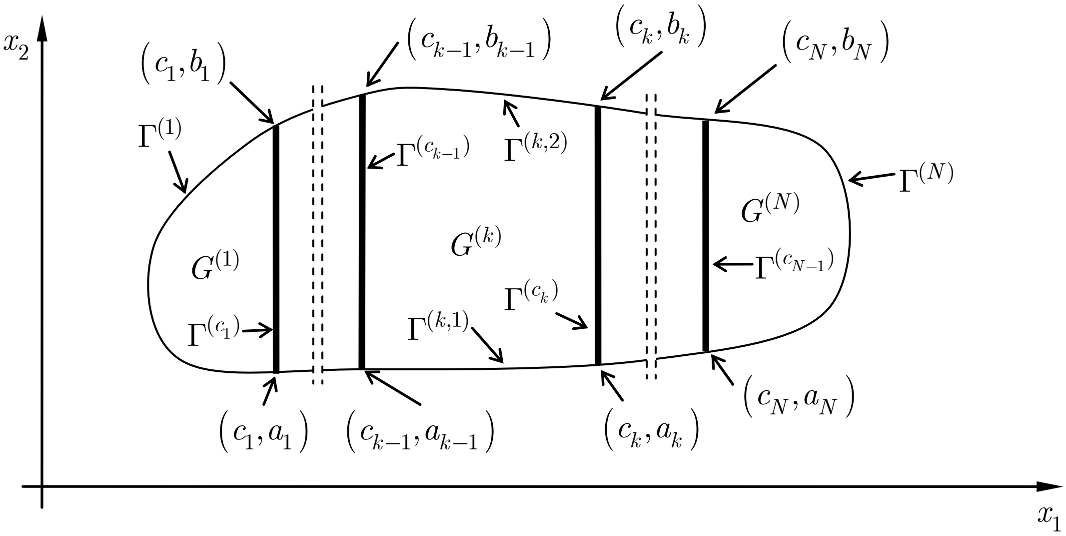

Figure 2: Domains and boundaries.

We also assume that the curves $\Gamma^{(k)}$ are described respectively by the smooth paths:

$$\gamma^{(k)}:\left[0,l^{(k)}\right]\rightarrow\mathbb{R}^2;\begin{cases}\gamma^{(k,1)}\left(s\right)=\left(\gamma_1^{(k,1)}\left(s\right),\gamma_2^{(k,1)}\left(s\right)\right),s\in\left[0,l^{(k,1)}\right],\\ \gamma^{(k,2)}\left(s\right)=\left(\gamma_1^{(k,2)}\left(s\right),\gamma_2^{(k,2)}\left(s\right)\right),s\in\left[0,l^{(k,2)}\right],\end{cases}\tag{4}$$

where: $k=1,2,\ldots,N$, $\gamma^{(1,2)}(s)\equiv 0,\gamma^{(N,2)}(s)\equiv 0$. From Eq. (3) and Eq. (4) it follows that $\gamma^{(k,i)}$ describes the arc $\Gamma^{(k,i)}$. In Eq. (4) s denotes the arc length measured from the point (c_{k-1},a_{k-1}) of the curve $\Gamma^{(k,1)}$ and from the point (c_k,b_k) of the curve $\Gamma^{(k,2)}$, $l^{(k,i)}=l(\Gamma^{(k,i)})$ is the length of the path $\gamma^{(k,i)}$ and $a_{k-1}=\gamma_2^{(k-1,1)}(l^{(k-1,1)}),b_k=\gamma_2^{(k,2)}(0)$.

The path which describes the boundary ∂G can be expressed as:

$$\gamma\left(s\right)=\begin{cases}\gamma^{(1,1)}\left(s\right)\text{ if } s\in\left[0,l^{(1,1)}\right],\\ \gamma^{(2,1)}\left(s-l^{(1,1)}\right)\text{ if } s\in\left[l^{(1,1)},l^{(1,1)}+l^{(2,1)}\right],\\ \ldots\\ \gamma^{(N-1,1)}\left(s-A_{N-2}\right)\text{ if } s\in\left[A_{N-2},A_{N-1}\right],\\ \gamma^{(N,1)}\left(s-A_{N-1}\right)\text{ if } s\in\left[A_{N-1},A_N\right],\\ \gamma^{(N-1,2)}\left(s-A_N\right)\text{ if } s\in\left[A_N,A_N+B_1\right],\\ \ldots\\ \gamma^{(2,2)}\left(s-A_N-B_{N-3}\right)\text{ if } s\in\left[A_N+B_{N-3},A_N+B_{N-2}\right],\end{cases}\tag{5}$$

where s denotes the arc length measured from the point (c_1,b_1) of the curve ∂G and

$$A_j=\sum_{i=1}^{j}l^{(i,1)},B_j=\sum_{i=1}^{j}l^{(N-i,2)},l=\sum_{i=1}^{N}\left(l^{(i,1)}+l^{(i,2)}\right),l^{(1,2)}=l^{(N,2)}=0.\tag{6}$$

It is well known that if $f:im(\beta)\rightarrow\mathbb{R}$, is a continuous function defined on the image Γ of a piecewise smooth path $\beta:\left[c,d\right]\rightarrow\mathbb{R}^2$, the curvilinear integral of f along Γ is given by:

$$\int_\Gamma f\left(x_1,x_2\right)ds=\int_c^d\left(f\circ\beta\right)(r)\left\|\beta'(r)\right\|dr,\tag{7}$$

where $\left(f\circ\beta\right)(r)=f\left(\beta\left(r\right)\right)$ and the norm $\left\|\beta'(r)\right\|$ is given by $\left(\beta_1'^2(r)+\beta_2'^2(r)\right)^{1/2}$. In the case of a real continuous function f defined on the image of the path γ (given by Eq.(5), i.e. the boundary curve $\partial\Omega$, the definition of Eq.(7) when s is taken as the parameter r, leads to:

$$\int_{\partial G}f\left(x_1,x_2\right)ds=\int_0^l\left(f\circ\gamma\right)(s)\left\|\gamma'(s)\right\|ds=\int_0^l\left(f\circ\gamma\right)(s)ds,\tag{8}$$

and

$$\int_{\partial G}f\left(x_1,x_2\right)ds=\sum_{i=1}^{2}\sum_{k=1}^{N}\int_{\Gamma^{(k,i)}}f\left(x_1,x_2\right)ds.\tag{9}$$

The additive property of Eq. (9) will prove be valuable in the definitions of functions and functionals over $\partial\Omega$, since they can be set up independently in each $\Gamma^{(k)}$ and by using Eq.(4). Thus, we assume that the rotational rigidities of the elastic restrains along the boundary are given by the functions:

$$r_R^{(k,i)} : im(\gamma^{(k,i)}) \to \mathbb{R},\ \ k = 1,2,\ldots,N, i = 1,2,\ r_R^{(c_k)} : im(\gamma^{(c_k)}) \to \mathbb{R}, \tag{10}$$

where $\gamma^{(c_k)}$ is the path which describes the line $\Gamma^{(c_k)}$. In the same manner the translational rigidities are given by the functions:

$$r_T^{(k,i)} : im(\gamma^{(k,i)}) \to \mathbb{R},\ \ k = 1,2,\ldots,N, i = 1,2,\ \ r_T^{(c_k)} : im(\gamma^{(c_k)}) \to \mathbb{R}. \tag{11}$$

It is obvious that $r_R^{(1,2)} \equiv 0, r_R^{(N,2)} \equiv 0, r_T^{(1,2)} \equiv 0$ and $r_T^{(N,2)} \equiv 0$.

In order to obtain a compact analytical scheme for the derivation of the boundary value problem which describes the dynamical behaviour of the mechanical system, we consider the following new procedure for the manipulation of derivatives introduced in Grossi (2011). Consider the well-known notation

$$D^{\alpha} u\left(\bar{x}\right) = \frac{\partial^{|\alpha|} u\left(\bar{x}\right)}{\partial x_1^{\alpha_1} \partial x_2^{\alpha_2} \partial x_3^{\alpha_3}}, \tag{12}$$

where $u : A \to \mathbb{R},\ u \in C^{|\alpha|}\left(A\right),\ A \subset \mathbb{R}^3$ and $\bar{x} = \left(x_1, x_2, x_3\right)$. The vector $\alpha = \left(\alpha_1, \alpha_2, \alpha_3\right)$ is a multi-index whose co-ordinates are non-negative integers and $\left|\alpha\right|$, is the sum $\left|\alpha\right| = \sum_{i=1}^{3} \alpha_i$. Now, introduce the following multi-indices:

$$\begin{gathered}\alpha^{(1)} = \left(2,0,0\right), \alpha^{(2)} = \left(0,2,0\right), \alpha^{(3)} = \left(1,1,0\right), \alpha^{(4)} = \left(0,0,2\right),\\ \mathbf{1}^{(i)} = \left(\delta_{1i}, \delta_{2i}, \delta_{3i}\right), i = 1,2,3,\end{gathered} \tag{13}$$

where δ_{ji} is the Kronecker delta, $\delta_{ji} = 1$ if $j = i$ and $\delta_{ji} = 0$ if $j \neq i$.

Consider a sufficiently smooth function $v : A \to \mathbb{R}$, defined on $A = G \times \left[0, T\right]$ for some fixed time $T > 0$, with $x = \left(x_1, x_2\right) \in G,\ x_3 = t,\ G \subset \mathbb{R}^2$. The use of Eq.(12) and Eq.(13) leads to

$$\begin{gathered}D^{\mathbf{1}^{(i)}} v\left(x,t\right) = \frac{\partial v}{\partial x_i}\left(x,t\right), \qquad D^{\alpha^{(i)}} v\left(x,t\right) = \frac{\partial^2 v}{\partial x_i^2}\left(x,t\right), i = 1,2,\\ D^{\alpha^{(3)}} v\left(x,t\right) = \frac{\partial^2 v}{\partial x_1 \partial x_2}\left(x,t\right), \quad D^{\mathbf{1}^{(3)}} v\left(x,t\right) = \frac{\partial v}{\partial t}\left(x,t\right),\\ D^{\alpha^{(4)}} v\left(x,t\right) = \frac{\partial^2 v}{\partial t^2}\left(x,t\right).\end{gathered} \tag{14}$$

The multi-indices of Eq. (13) verify the following algebraic rules, (Grossi, 2011):

$$\mathbf{1}^{(i)} + \mathbf{1}^{(i)} = \alpha^{(i)}, \mathbf{1}^{(3-i)} + \mathbf{1}^{(i)} = \alpha^{(3)},\ \forall i \in \left\{1,2\right\}, \mathbf{1}^{(3)} + \mathbf{1}^{(3)} = \alpha^{(4)}. \tag{15}$$

Let us consider the following notation: $C^n\left(S\right)$ denotes the set of all real functions $u : G \to \mathbb{R}$ that have continuous partial derivatives of orders n and $C^n\left(\bar{S}\right)$ denotes the set of all $u \in C^n\left(S\right)$ for which all partial derivatives of order n can be extended continuously to the closure $\bar{S}$ of S. A essential step to compact analytical expressions, is the derivation of formulae needed to transform the terms which involves derivatives of variations. Let us suppose that

$$\begin{aligned}&S_i^{(k)}: A \to \mathbb{R}, v: A \to \mathbb{R}, A = G \times \left[0, T\right], S_i^{(k)}\left(\bullet, t\right), v\left(\bullet, t\right) \in C^2(\bar{G}),\\&n_i^{(k)}: \partial\Omega^{(k)} \to \mathbb{R},\ i \in \left\{1, 2\right\},\ k \in \left\{1, 2, \ldots, N\right\}.\end{aligned} \tag{16}$$

Then, the following formulas are valid:

$$\begin{aligned}&\int_{G^{(k)}} S_i^{(k)}\left(x,t\right) D^{\alpha^{(i)}} v\left(x,t\right) dx = \int_{\partial G^{(k)}} \Big[S_i^{(k)}\left(x,t\right)\left(D^{\mathbf{1}^{(i)}} v\left(x,t\right)\right) n_i^{(k)}\left(x\right)\\&-\left(D^{\mathbf{1}^{(i)}} S_i^{(k)}\left(x,t\right)\right) v\left(x,t\right) n_i^{(k)}\left(x\right)\Big] + \int_{G^{(k)}} \left(D^{\alpha^{(i)}} S_i^{(k)}\left(x,t\right)\right) v\left(x,t\right) dx,\end{aligned} \tag{17}$$

$$\begin{aligned}&\int_{G^{(k)}} S_i^{(k)}\left(x,t\right) D^{\alpha^{(3)}} v\left(x,t\right) dx\\&= \frac{1}{2}\sum_{i=1}^{2}\Big\{\int_{\partial G^{(k)}}\Big[S_i^{(k)}\left(x,t\right)\left(D^{\mathbf{1}^{(3-i)}} v\left(x,t\right)\right) n_i^{(k)}\left(x\right)\\&-\left(D^{\mathbf{1}^{(i)}} S_i^{(k)}\left(x,t\right)\right) v\left(x,t\right) n_{3-i}^{(k)}\left(x\right)\Big] ds\Big\} + \int_{G^{(k)}}\left(D^{\alpha^{(3)}} S_i^{(k)}\left(x,t\right)\right) v\left(x,t\right) dx,\end{aligned} \tag{18}$$

where $n_i^{(k)}$ denotes the $i-$th component of the outward unit normal $\vec{n}^{(k)}$ to the boundary $\partial\Omega^{(k)}$. The demonstrations of Eq. (17) and Eq. (18) are a direct consequence of the proposition 2 of Grossi (2011).

Hamilton´s principle requires that between times t_0 and t_1, at which the positions of the mechanical system are known, it should execute a motion which makes stationary the functional $F(w) = \int_{t_0}^{t_1}\left(E_K - E_D\right) dt$, on the space of admissible functions. From the well known expressions of the kinetic and potential energies of the mechanical system under study, it follows that the energy functional is given by

$$\begin{aligned}F\left(w\right) = \frac{1}{2}\int_{t_0}^{t_1}\Bigg\{&\sum_{k=1}^{N}\Bigg[\int_{G^{(k)}}\Bigg(\left(\rho h\right)^{(k)}\left(\frac{\partial w}{\partial t}\right)^2 - C_{11}^{(k)}\left(\frac{\partial^2 w}{\partial x_1^2}\right)^2\\&-2C_{12}^{(k)}\frac{\partial^2 w}{\partial x_1^2}\frac{\partial^2 w}{\partial x_2^2} - C_{22}^{(k)}\left(\frac{\partial^2 w}{\partial x_2^2}\right)^2 - 4\frac{\partial^2 w}{\partial x_1 \partial x_2}\left(C_{16}^{(k)}\frac{\partial^2 w}{\partial x_1^2} + C_{26}^{(k)}\frac{\partial^2 w}{\partial x_2^2}\right)\\&-4C_{66}^{(k)}\left(\frac{\partial^2 w}{\partial x_1 \partial x_2}\right)^2 + 2q^{(k)} w\Bigg) dx\\&-\sum_{i=1}^{2}\int_{\Gamma^{(k,i)}}\left(r_T^{(k,i)} w^2 + r_R^{(k,i)}\left(\frac{\partial w}{\partial \vec{n}^{(k)}}\right)^2\right) ds\Bigg] - E_h\Bigg\} dt,\end{aligned} \tag{19}$$

where: $w = w(x,t)$, $C_{lm}^{(k)} = C_{lm}^{(k)}(x)$ are the rigidities of the anisotropic material (Lekhnitskii, 1968), $\partial w / \partial \vec{n}^{(k)}$ is the directional derivative of w with respect to the outward normal unit vector $\vec{n}^{(k)}$ to the curve $\Gamma^{(k)}$,

$$E_h = \sum_{k=1}^{N-1} \int_{\Gamma^{(c_k)}} \left(r_T^{(c_k)} w^2 + r_R^{(c_k)} \left(\left[\partial w / \partial x_1 \right]_{c_k} \right)^2 \right) ds \tag{20}$$

and the symbol $\left[\partial w / \partial x_1 \right]_{c_k}$, denotes the difference of lateral derivatives

$$\left[\frac{\partial w}{\partial x_1} \right]_{c_k} = \frac{\partial w}{\partial x_1}\left(c_k^+, x_2, t\right) - \frac{\partial w}{\partial x_1}\left(c_k^-, x_2, t\right). \tag{21}$$

The definition of the variation of F at w in the direction v, is given by

$$\delta F(w;v) = \frac{dF}{d\varepsilon}(w + \varepsilon v)\Big|_{\varepsilon=0}, \tag{22}$$

and the condition of stationary functional requires that

$$\delta F(w;v) = 0, \forall v \in D_a \tag{23}$$

where D_a is the space of admissible directions at w for the domain D of this functional. In order to make the mathematical developments required by the application of the techniques of the calculus of variations, we assume that:

$$\begin{aligned} &(\rho h)^{(k)} \in C\left(\bar{G}^{(k)}\right), q^{(k)}(\bullet, t) \in C\left(\bar{G}^{(k)}\right), E_{lm}^{(k)} \in C^2\left(\bar{G}^{(k)}\right), w(x, \bullet) \in C^2\left[t_0, t_1\right], \\ &w(\bullet, t) \in C\left(\bar{G}\right), w(\bullet, t)\Big|_{\bar{G}^{(k)}} \in C^4\left(\bar{G}^{(k)}\right), \bar{G}^{(k)} = G^{(k)} \cup \partial G^{(k)}, k = 1, 2, \ldots, N, \end{aligned} \tag{24}$$

It must be noted that as a consequence of the presence of the lines hinges, the derivative $\partial w / \partial x_1$ and the corresponding derivatives of greater order, do not necessarily exist in the domain G, so it is necessary to impose the conditions $w(\bullet, t)\Big|_{\bar{G}^{(k)}} \in C^4\left(\bar{G}^{(k)}\right)$, $k = 1, 2, \ldots, N$.

In view of all these observations and since Hamilton's principle requires that at times t_0 and t_1 the positions are known, the space D is given by

$$\begin{aligned} D = \Big\{ &w; w(x, \bullet) \in C^2\left[t_0, t_1\right], w(\bullet, t) \in C\left(\bar{G}\right), w(\bullet, t)\Big|_{\bar{G}^{(k)}} \in C^4\left(\bar{G}^{(k)}\right), \\ &k = 1, \ldots, N, w(x, t_0), w(x, t_1) \text{ prescribed} \Big\}. \end{aligned} \tag{25}$$

The only admissible directions v at $w \in D$ are those for which $w + \varepsilon v \in D$ for all sufficiently small ε and $\delta F(w;v)$ exists. In consequence, and in view of Eq. (25), v is an admissible direction at w for D if, and only if, $v \in D_a$ where

$$D_a = \left\{ v; v\left(x,\bullet\right) \in C^2\left[t_0,t_1\right], v\left(\bullet,t\right) \in C\left(\bar{G}\right), v\left(\bullet,t\right)\Big|_{\bar{G}^{(k)}} \in C^4\left(\bar{G}^{(k)}\right), \right.$$
$$\left. i = 1,\ldots,2, v\left(x,t_0\right) = v\left(x,t_1\right) = 0, \forall x \in \bar{G} \right\}. \tag{26}$$

3 RECTANGULAR ANISOTROPIC PLATES

Considering a rectangular anisotropic plate with:

$$G = \left\{ \left(x_1,x_2\right), 0 < x_1 < a, 0 < x_2 < b \right\}, \tag{27}$$

and three lines hinges parallel to the x_2 axis.

Consequently the corresponding sub domains are given by:

$$G^{(i)} = \left\{ \left(x_1,x_2\right), c_{i-1} < x_1 < c_i, 0 < x_2 < b \right\}, i = 1,\ldots,4, \tag{28}$$

where $c_0 = 0$ and $c_4 = a$.

The curves $\Gamma^{(k)}$ described by Eq. (3) in this case are given by:

$$\begin{aligned}
&\Gamma^{(k,1)} = \left\{ \left(c_{k-1} + x_1, 0\right),\ x_1 \in \left[0, c_k - c_{k-1}\right] \right\}, k = 2,3, \\
&\Gamma^{(k,2)} = \left\{ \left(c_k - x_1, b\right),\ x_1 \in \left[0, c_k - c_{k-1}\right] \right\}, k = 2,3, \\
&\Gamma^{(1,1)} = \left\{ \left(c_1 - x_1, b\right),\ x_1 \in \left[0, c_1\right] \right\}, \Gamma^{(1,2)} = \left\{ \left(0, b - x_2, b\right),\ x_2 \in \left[0, b\right] \right\}, \\
&\Gamma^{(1,3)} = \left\{ \left(x_1, 0\right),\ x_1 \in \left[0, c_1\right] \right\}, \\
&\Gamma^{(4,1)} = \left\{ \left(c_3 + x_1, 0\right),\ x_1 \in \left[0, a - c_3\right] \right\}, \Gamma^{(4,2)} = \left\{ \left(a, x_2\right),\ x_2 \in \left[0, b\right] \right\}, \\
&\Gamma^{(4,3)} = \left\{ \left(a - x_1, b\right),\ x_1 \in \left[0, a - c_3\right] \right\},
\end{aligned} \tag{29}$$

where the following notation has been adopted:

$$\Gamma^{(1)} = \Gamma^{(1,1)} \cup \Gamma^{(1,2)} \cup \Gamma^{(1,3)}, \tag{30}$$

and (see Figure 3)

$$\Gamma^{(4)} = \Gamma^{(4,1)} \cup \Gamma^{(4,2)} \cup \Gamma^{(4,3)}. \tag{31}$$

It must be noted that the upper sides of the plate are given by (see Figure 3):

$$\Gamma^{(k,j)}, \left(k,j\right) \in \left\{ \left(1,1\right), \left(2,2\right), \left(3,2\right), \left(4,3\right) \right\} \tag{32}$$

which correspond $\tilde{n}_1^{(k)} = 0$, $\tilde{n}_2^{(k)} = 1$, meanwhile the lower sides of the plate are given by

$$\left(k,j\right) \in \left\{ \left(1,3\right), \left(2,1\right), \left(3,1\right), \left(4,1\right) \right\} \tag{33}$$

and $\tilde{n}_1^{(k)} = 0$, $\tilde{n}_2^{(k)} = -1$.

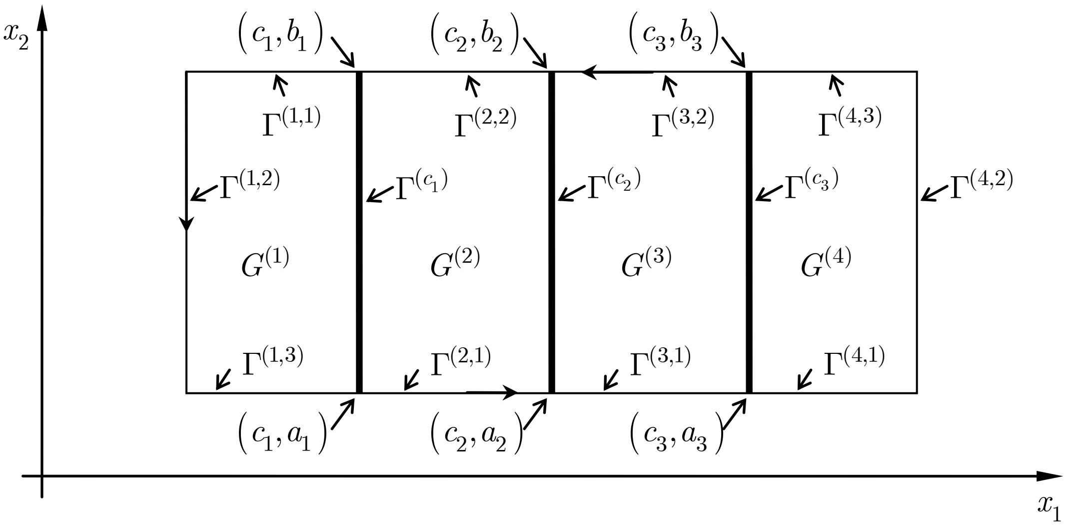

Figure 3: Rectangular plate with three internal lines hinges

From the development of the Calculus of Variations of the energy functional the following relations are obtained:

$$\begin{aligned} D^{\mathbf{1}^{(1)}} w\left(x_1,x_2,t\right)\Big|_{\Gamma^{(k,j)}} &= -D^{\mathbf{1}^{(2)}} \tilde{w}\left(0,y_2,t\right), \\ D^{\mathbf{1}^{(2)}} w\left(x_1,x_2,t\right)\Big|_{\Gamma^{(k,j)}} &= D^{\mathbf{1}^{(1)}} \tilde{w}\left(0,y_2,t\right) \end{aligned} \tag{34}$$

when $\left(k,j\right) \in \left\{\left(1,1\right),\left(2,2\right),\left(3,2\right),\left(4,3\right)\right\}$ and

$$\begin{aligned} D^{\mathbf{1}^{(1)}} w\left(x_1,x_2,t\right)\Big|_{\Gamma^{(k,j)}} &= D^{\mathbf{1}^{(2)}} \tilde{w}\left(0,y_2,t\right), \\ D^{\mathbf{1}^{(2)}} w\left(x_1,x_2,t\right)\Big|_{\Gamma^{(k,j)}} &= -D^{\mathbf{1}^{(1)}} \tilde{w}\left(0,y_2,t\right) \end{aligned} \tag{35}$$

when $\left(k,j\right) \in \left\{\left(1,3\right),\left(2,1\right),\left(3,1\right),\left(4,1\right)\right\}$. Finally we have

$$\begin{aligned} D^{\mathbf{1}^{(1)}} w\left(x_1,x_2,t\right)\Big|_{\Gamma^{(1,2)}} &= -D^{\mathbf{1}^{(1)}} \tilde{w}\left(0,y_2,t\right), \\ D^{\mathbf{1}^{(2)}} w\left(x_1,x_2,t\right)\Big|_{\Gamma^{(1,2)}} &= -D^{\mathbf{1}^{(2)}} \tilde{w}\left(0,y_2,t\right), \\ D^{\mathbf{1}^{(1)}} w\left(x_1,x_2,t\right)\Big|_{\Gamma^{(4,2)}} &= D^{\mathbf{1}^{(1)}} \tilde{w}\left(0,y_2,t\right), \\ D^{\mathbf{1}^{(2)}} w\left(x_1,x_2,t\right)\Big|_{\Gamma^{(4,2)}} &= D^{\mathbf{1}^{(2)}} \tilde{w}\left(0,y_2,t\right). \end{aligned} \tag{36}$$

In analogue manner we have

$$\tilde{r}_R^{(k,j)}\left(0,y_2\right) D^{\mathbf{1}^{(1)}} \tilde{w}\left(0,y_2,t\right) = -\tilde{S}_2^{(k)}\left(0,y_2,t\right), \tag{37}$$

when $\left(k,j\right) \in \left\{\left(1,1\right),\left(2,2\right),\left(3,2\right),\left(4,3\right)\right\}$ and

$$\tilde{r}_R^{(k,j)}\left(0,y_2\right) D^{\mathbf{1}^{(1)}} \tilde{w}\left(0,y_2,t\right) = -\tilde{S}_2^{(k)}\left(0,y_2,t\right), \tag{38}$$

when $(k,j)\in\{(1,3),(2,1),(3,1),(4,1)\}$.

where

$$S_i^{(k)}=\sum_{j=1}^{3}A_{ij}^{(k)}(x)D^{\alpha^{(j)}}w(x,t), \tag{39}$$

with the coefficients $A_{ij}^{(k)}$ as elements of the symmetric matrix

$$\mathbf{A}=\begin{pmatrix} C_{11}^{(k)} & C_{12}^{(k)} & 2C_{16}^{(k)} \\ C_{12}^{(k)} & C_{22}^{(k)} & 2C_{26}^{(k)} \\ 2C_{16}^{(k)} & 2C_{26}^{(k)} & 4C_{66}^{(k)} \end{pmatrix}. \tag{40}$$

Finally for the remaining two sides we have:

$$\tilde{r}_R^{(1,2)}(0,y_2)D^{\mathbf{1}^{(1)}}\tilde{w}(0,y_2,t)=-\tilde{S}_1^{(1)}(0,y_2,t), \tag{41}$$

and

$$\tilde{r}_R^{(4,2)}(0,y_2)D^{\mathbf{1}^{(1)}}\tilde{w}(0,y_2,t)=-\tilde{S}_1^{(4)}(0,y_2,t). \tag{42}$$

Let us consider the first of Eqs. (37). From Eq. (34) and the relations between the derivatives of order two lead to the following boundary condition:

$$r_R^{(1,1)}(x)D^{\mathbf{1}^{(2)}}w(x,t)\Big|_{\Gamma^{(1,1)}}=-\sum_{j=1}^{3}A_{ij}^{(1)}(x)D^{\alpha^{(j)}}w(x,t). \tag{43}$$

From Eq. (40) it is immediate that Eq. (43) in the classical notation is given by:

$$\begin{aligned} &r_R^{(1,1)}(x_1,x_2)\frac{\partial w}{\partial x_2}(x_1,x_2,t)=-C_{12}^{(1)}(x_1,x_2)\frac{\partial^2 w}{\partial x_1^2}(x_1,x_2,t) \\ &-C_{22}^{(1)}(x_1,x_2)\frac{\partial^2 w}{\partial x_2^2}(x_1,x_2,t)-2C_{26}^{(1)}(x_1,x_2)\frac{\partial^2 w}{\partial x_1\partial x_2}(x_1,x_2,t), \end{aligned} \tag{44}$$

and analog expressions correspond to the other sides.

4 THE RITZ AND LAGRANGE MULTIPLIERS METHOD

The transition conditions (45) obtained from the calculus of variations from the energy functional shown in Eq.(19), ensure the continuity of the transverse deflection along the internal lines hinges.

$$\begin{aligned} &w(c_k^-,x_2,t)=w(c_k^+,x_2,t)=w(c_k,x_2,t),x_2\in[a_k,b_k], \\ &k=1,2,\ldots,N-1. \end{aligned} \tag{45}$$

Since it is difficult to construct a simple and adequate deflection function which can be applied to the entire plate, and to show the continuity of displacement and the discontinuities of the slope crossing the lines hinges, the Ritz method is used in conjunction with the Lagrange multiplier method to force the continuity along the lines hinges by means of a suitable Lagrange multipliers (Quintana and Grossi, 2012). When the plate makes free vibrations, the displacements of the plate are given by harmonic functions of the time, i.e.

$$w^{(k)}\left(x,y,t\right)=W^{(k)}\left(x,y\right)\cos\omega t,\ k=1,2,\ldots,N, \tag{46}$$

where ω is the radian frequency of the plate. Substituting Eq. (46) into Eq. (19) the Lagrange multipliers method requires the stationarity of the functional

$$I_G=F_{\max}+R, \tag{47}$$

where R is the subsidiary condition which imposes the transition conditions shown in Eq.(45). In the present paper the transverse deflections for rectangular plates are represented by means of

$$\begin{aligned}&W^{(k)}\left(x_1,x_2\right)=\sum_{i=1}^{m_k}\sum_{j=1}^{n_k}a_{ij}^{(k)}p_i^{(k)}\left(x_1\right)q_j^{(k)}\left(x_2\right),\ k=1,2,\\&x_1=x_1\,/\,a, x_2=x_2\,/\,b,\end{aligned} \tag{48}$$

where a and b are the side lengths of the plate, $p_i^{(k)},q_i^{(k)}$ are polynomials. The application of the Ritz method in conjunction with the Lagrange multipliers methods leads to the following governing eigenvalue equation (Quintana and Grossi, 2012):

$$\left(\left[\mathrm{K}\right]\text{-}\Omega^2\left[\mathrm{M}\right]\right)\left\{a\right\}=\left\{0\right\}, \tag{49}$$

where $\Omega=\omega b^2\sqrt{\rho h/D}$ is the non-dimensional frequency parameter. For sake of simplicity $D^{(k)}=D,\ h^{(k)}=h, k=1,2,\ldots,N$ has been adopted.

4.1 Convergence and comparison of eigenvalues and modal shapes

In order to establish the accuracy and applicability of the approach developed and discussed in the previous sections, numerical results were computed for a number of plate problems for which comparison values were available in the literature and also convergence studies have been implemented. Additionally, new numerical results were generated for rectangular plates with one or more internal lines hinges and different boundary conditions. All calculations have been performed taking Poisson's ratio $\mu=0.3$. To describe the boundary conditions the following nomenclature is used, e.g. for a plate with boundary conditions SFCF correspond to Edge $\Gamma^{(1,2)}$ simply supported, Edge $\Gamma^{(4,2)}$ free, Edge $\Gamma^{(1,3)}\cup\Gamma^{(2,1)}\cup\Gamma^{(3,1)}\cup\Gamma^{(4,1)}$ clamped, and Edge $\Gamma^{(1,1)}\cup\Gamma^{(2,2)}\cup\Gamma^{(3,2)}\cup\Gamma^{(4,3)}$ free (see Figure 3).

Results of a convergence study of the values of the frequency parameter $\Omega=\omega b^2\sqrt{\rho h\,/\,D}$ are presented in Table 1. The first six values of Ω are presented for a square SSSS plate with an internal line hinge located at two different positions, namely, $\overline{c}_1=0.3$ and $\overline{c}_1=0.5$ where $\overline{c}=c\,/\,a$ is the hinge location. The convergence of the mentioned frequency parameters is studied by gradually increasing the number of polynomial in the approximate functions $W^{(1)}$, $W^{(2)}$ and the Lagrange multiplier $\lambda=\lambda(y)$. It can be observed that the frequency parameters converge monotonically from above as the number of terms increases and the values obtained with N terms agree with the values reported in Quintana and Grossi (2012).

		Mode Sequence					
$\bar{c}$	N	1	2	3	4	5	6
0.3	4	16.79228	39.09601	47.57494	72.15651	97.65285	127.74591
	5	16.78916	39.08796	47.56763	72.12600	96.43386	98.21747
	6	16.78915	39.08628	47.42135	72.01026	96.30013	98.21611
	7	16.78915	39.08628	47.42135	72.01025	96.29318	96.80383
	8	16.78915	39.08628	47.42073	72.00980	96.29287	96.80383
	9	16.78915	39.08628	47.42073	72.00980	96.29286	96.78357
	10	16.78915	39.08628	47.42073	72.00980	96.29286	96.78357
	11	16.78915	39.08628	47.42073	72.00980	96.29286	96.78347
	Reference	16.78915	39.08628	47.42073	72.0098	96.29286	96.78357
0.5	4	16.14205	46.92498	49.45364	75.71555	79.13290	111.98548
	5	16.13485	46.88817	49.35421	75.40041	79.06601	97.49206
	6	16.13478	46.73884	49.34806	75.28386	78.95728	97.47892
	7	16.13478	46.73877	49.34802	75.28341	78.95725	96.06101
	8	16.13478	46.73815	49.34802	75.28338	78.95684	96.06096
	9	16.13478	46.73815	49.34802	75.28338	78.95684	96.04060
	10	16.13478	46.73815	49.34802	75.28338	78.95684	96.04060
	11	16.13478	46.73815	49.34802	75.28338	78.95684	96.04051
	Reference	16.13478	46.73815	49.34802	75.28338	78.95684	96.0406

Table 1. Convergence study of the first six values of the frequency parameter Ω for an isotropic square SSSS plate with an internal line hinge located a $\bar{c} = 0.3$ and $\bar{c} = 0.5$. Reference: Quintana and Grossi (2012)

Table 2 depicts a comparison with the values obtained in Quintana and Grossi (2012) of the first six values of the frequency parameter Ω for CSFF rectangular isotropic plates with $b / a = 1 / 2$ and $b / a = 1 / 3$ and with an internal line hinge located at different positions. The agreement observed is excellent.

b / a	$\bar{c}$	Reference	Mode sequence					
			1	2	3	4	5	6
1/2	1/3	Present	3.51514	7.68667	8.21521	16.48131	23.84325	26.59203
		Reference	3.51554	7.68729	8.21567	16.48237	23.84415	26.5944
	1/2	Present	2.23656	7.49759	11.37571	18.02734	19.13566	26.52157
		Reference	2.23689	7.49831	11.37617	18.02897	19.13922	26.52227
	2/3	Present	1.50111	7.51734	10.04917	17.09403	24.69761	26.37444
		Reference	1.5014	7.51825	10.05115	17.09667	24.69953	26.37498
1/3	1/3	Present	1.55388	3.63465	4.77940	10.02915	10.58447	17.30755
		Reference	1.55403	3.63483	4.77971	10.02977	10.58499	17.30863
	1/2	Present	0.98822	4.74937	5.02554	8.52496	10.42039	16.30504
		Reference	0.98842	4.74981	5.02579	8.52647	10.42137	16.3068
	2/3	Present	0.66315	4.44705	4.75928	10.16342	10.99039	14.99425
		Reference	0.66334	4.44817	4.75985	10.16473	10.9914	14.99632

Table 2. Comparison of the first six values of the frequency parameter Ω for CSFF rectangular isotropic plates with $b / a = 1 / 2$ and $b / a = 1 / 3$ with an internal line hinge located at different positions with the values obtained in Quintana and Grossi (2012).

Table 3 gives the first four values of the frequency parameter Ω for a CCCC anisotropic square plate with different values of the dimensionless rotational restriction R_{12} of the first hinge and R_{23} of the second hinge located at $\bar{c}_1 = 0.25$ and $\bar{c}_2 = 0.75$ respectively. The modal shapes shown correspond to $R_{12} = R_{23} = 0$ and $R_{12} = R_{23} = \infty$, these last values are compared with the ones obtained in Grossi (2001). The plate anisotropy is $D_{11} = 1$, $D_{22} = 0.1$, $D_{66} = 0.0247750$, $D_{12} = 0.03$, $D_{16} = D_{26} = 0$.

R_{12}	R_{23}	Mode sequence			
		1	2	3	4
0	0	23.45956	30.56252	37.85855	44.15721
		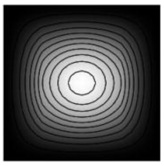	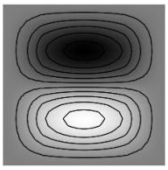	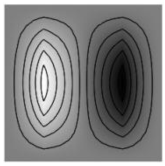	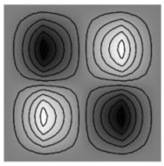
10	0	23.61956	30.75000	44.68048	45.98426
1000	0	23.64241	30.77948	45.97679	46.06113
∞	0	23.64268	30.77983	45.98424	46.07002
∞	10	23.92261	31.09512	46.34815	59.35300
∞	1000	23.96589	31.14802	46.40945	62.73310
∞	∞	23.96640	31.14865	46.41019	62.77503
		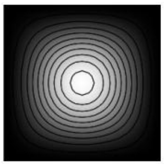	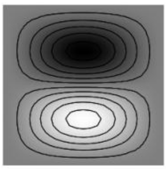	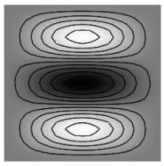	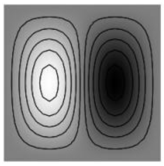
Reference		23.96642	31.14868	46.4672	62.77512

Table 3. First four values of the frequency parameter Ω for a CCCC anisotropic square plate with different values of the dimensionless rotational restriction R_{12} of the first hinge and R_{23} of the second hinge located at $\bar{c}_1 = 0.25$ and $\bar{c}_2 = 0.75$ respectively, the modal shapes shown correspond to $R_{12} = R_{23} = 0$ and $R_{12} = R_{23} = \infty$, these last values are compared with the ones obtained in the Reference: Grossi (2001). The plate anisotropy is $D_{11} = 1$, $D_{22} = 0.1$, $D_{66} = 0.0247750$, $D_{12} = 0.03$, $D_{16} = D_{26} = 0$.

4.2 New numerical results

Table 4 presents the first six values of the frequency parameter Ω for a SSSS anisotropic rectangular plate with two internal hinges, with $b/a = 1/2$ and $b/a = 2$, with the dimensionless translational restriction $T_{12} = T$, located at the first hinge, at $\bar{c}_1 = 0.25$, and $T_{23} = T$ located at the second hinge at $\bar{c}_2 = 0.5$ and 0.75. The plate anisotropy considered is $D_{11} = 1$, $D_{22} = 0.2482224$, $D_{66} = 0.3361177$, $D_{12} = 0.3448467$, $D_{16} = -0.495691$, $D_{26} = -0.155368$.

Figure 4 shows the first five values of the frequency parameter Ω and modal shapes contour lines of a FFCS anisotropic rectangular plate with two internal hinges, located at $\bar{c}_1 = 1/3$ and $\bar{c}_2 = 2/3$, with $b/a = 1/2$ and $b/a = 2$. The plate anisotropy considered is $D_{11} = 1$, $D_{22} = 0.115202317$, $D_{66} = 0.0948810$, $D_{12} = 0.100812496$, $D_{16} = -0.24333539$, $D_{26} = -0.0120837$.

b/a	$\bar{c}_2$	T	Mode Sequence					
			1	2	3	4	5	6
1/2	0.5	0	6.13272	11.37277	18.17580	20.13500	27.30896	32.08927
		10	7.63488	12.38857	18.76423	20.69716	27.73055	32.33768
		100	12.88142	18.08172	23.62405	25.12977	31.00894	34.83498
		1000	14.91485	27.64070	35.54541	40.42164	43.09226	45.16699
		10000	15.12288	28.18826	42.68467	43.41719	45.13909	46.85752
	0.75	0	6.32794	10.19099	19.72051	20.31024	27.14421	32.91900
		10	7.47868	11.53123	20.19905	20.80931	27.70484	33.09273
		100	11.81817	18.86774	24.36218	24.50014	32.08935	34.73187
		1000	14.68894	27.11056	38.34673	39.06688	42.42447	44.69072
		10000	15.09332	28.12712	43.22336	43.23943	44.93227	46.73932
2	0.5	0	14.99106	33.44484	35.48624	57.75759	72.83382	88.92077
		10	17.37731	34.60772	37.26786	58.44827	73.68858	89.38113
		100	31.36994	43.56466	50.56603	64.28163	80.93638	93.39404
		1000	83.40285	90.06103	103.14080	116.25158	124.56296	130.59208
		10000	150.03590	159.29239	176.02018	201.02375	234.35466	276.83000
	0.75	0	15.07049	29.55181	34.56451	56.57771	65.37057	87.86891
		10	16.97118	31.28123	35.66269	57.20247	66.22118	88.26760
		100	28.76254	41.22825	46.70113	62.33214	73.55855	91.71980
		1000	73.87318	80.81618	94.81841	112.35227	118.07792	125.83710
		10000	141.62027	149.97440	165.31486	188.57398	220.05158	261.18673

Table 4. First six values of the frequency parameter Ω for a SSSS anisotropic rectangular plate with two internal hinges, located at $\bar{c}_1 = 0.25$ and $\bar{c}_2 = 0.5$ and 0.75, with $b/a = 1/2$ and $b/a = 2$, with the dimensionless translational restriction $T_{12} = T,$ located at the first hinge, at $\bar{c}_1 = 0.25$, and $T_{23} = T$ located at the second hinge, $\bar{c}_2 = 0.5$ and 0.75. The plate anisotropy considered is $D_{11} = 1,\ D_{22} = 0.2482224,\ D_{66} = 0.3361177,$ $D_{12} = 0.3448467,\ D_{16} = -0.495691,\ D_{26} = -0.155368.$

b/a	Mode sequence				
	1	2	3	4	5
1/2	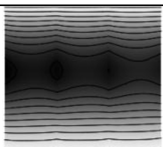	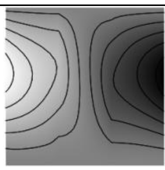	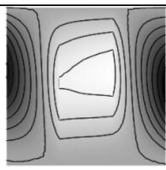	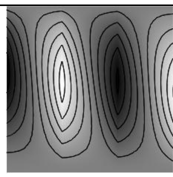	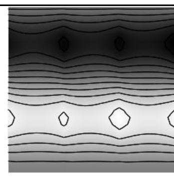
	5.07587429	5.79203293	7.89533066	9.991669568	16.49430191
2	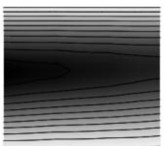	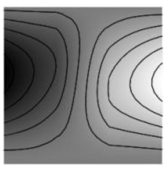	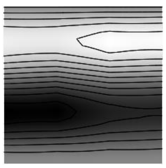	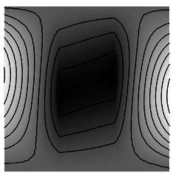	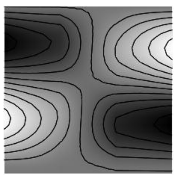
	4.99314088	10.0006422	16.2635517	19.68378208	23.75561997

Figure 4. First five values of the frequency parameter Ω and modal shapes contour lines of a FFCS anisotropic rectangular plate with two internal hinges, located at $\bar{c}_1 = 0.33$ and $\bar{c}_2 = 0.66$ with $b/a = 1/2$ and $b/a = 2$ The plate anisotropy considered is $D_{11} = 1,\ D_{22} = 0.115202317,\ D_{66} = 0.0948810,\ D_{12} = 0.100812496,$ $D_{16} = -0.24333539,\ D_{26} = -0.0120837.$

Figure 5 shows the first five values of the frequency parameter Ω and modal shapes contour lines of a FFCS anisotropic rectangular plate with three internal hinges, located at $\bar{c}_1 = 0.3$, $\bar{c}_2 = 0.3$, and $\bar{c}_3 = 0.9$, with $b/a = 1/2$ and $b/a = 2$. The plate anisotropy considered is $D_{11} = 1$, $D_{22} = 0.115202317$, $D_{66} = 0.0948810$, $D_{12} = 0.100812496$, $D_{16} = -0.24333539$, $D_{26} = -0.0120837$.

b/a	Mode sequence				
	1	2	3	4	5
1/2	5.06333355	5.711700994	7.591103	10.0988422	15.73005937
	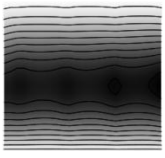	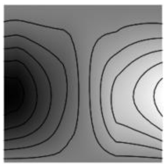	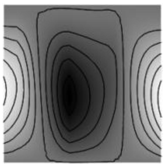	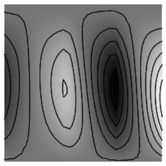	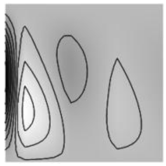
2	4.988601252	9.833599991	16.24223254	18.63116706	23.38073109
	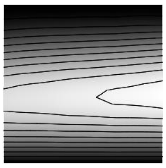	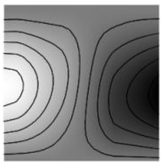	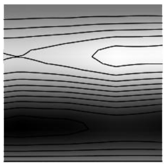	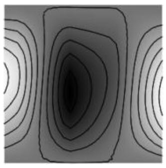	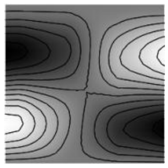

Figure 5. First five values of the frequency parameter Ω and modal shapes contour lines of a FFCS anisotropic rectangular plate with three internal hinges, located at $\bar{c}_1 = 0.3$, $\bar{c}_2 = 0.3$, and $\bar{c}_3 = 0.9$, with $b/a = 1/2$ and $b/a = 2$. The plate anisotropy considered is $D_{11} = 1$, $D_{22} = 0.115202317$, $D_{66} = 0.0948810$, $D_{12} = 0.100812496$, $D_{16} = -0.24333539$, $D_{26} = -0.0120837$.

5 CONCLUSIONS

This paper presents the formulation of an analytical model for the dynamic behavior of anisotropic plates, with several arbitrarily located internal lines hinges with elastics supports and piecewise-smooth boundaries elastically restrained against rotation and translation. The equations of motion and its associated boundary and transition conditions were derived handling Hamilton's principle in a rigorous framework.

An approach to the solution of the natural vibration problems, of the mentioned plates by a direct variational method, has been presented. A simple, computationally efficient and accurate algorithm has been developed for the determination of frequencies and modal shapes of natural vibrations. The approach is based on a combination of the Ritz method and the Lagrange multipliers method. Sets of parametric studies have been performed to show the influence of the line hinge and its location on the vibration behaviors.

REFERENCES

Blanchard, P., and Brüning, E., *Variational Methods in Mathematical Physics*, Springer-Verlag, 1992.

Bliss, G., *Calculus of Variations*, The Mathematical Association of América. The Open Court Publ. Co., 1971.

Brechtken-Manderscheid, U., *Introduction to the Calculus of Variations*, Chapman and Hall London, 1991.

Courant, R., and Hilbert, D. *Methods of Mathematical Physics*, Interscience Publ., 1953.

Dym, C., Shames, I., *Solid Mechanics: A Variational Approach*, Mc Graw Hill Book Co., 1973.

Ewing, G. M., *Calculus of Variations with Applications*, Dover Publications, 1985.

Giaquinta M., and Hildebrandt, S., *Calculus of Variations I*, Springer-Verlag, 1996.

Grossi, R. O., On the existence of weak solutions in the study of anisotropic plates, *Journal of sound and Vibration*, 242(3):542-552, 2001.

Grossi, R. O., *Cálculo de Variaciones. Teoría y aplicaciones*, Centro Internacional de Métodos Numéricos en Ingeniería (CIMNE) Editorial Dsignum, 2010.

Grossi, R. O., A Note on the use of variational methods for treatment of plate dynamics, *Journal of Multi-body Dynamics,* Part K, 225: 263-271, 2011.

Grossi, R. O., Boundary value problems for anisotropic plates with internal line hinges, *Acta Mechanica*, 223: 125-144, 2012.

Guelfand I., and Fomin, S., *Calculus of Variations*, Prentice Hall, 1963.

Gupta, P. R., and Reddy, J.N., Buckling and vibrations of orthotropic plates with an internal line hinge, *International Journal of Structural Stability and Dynamics*, 2(4):457-486, 2002.

Huang, M., Ma, X. Q., Sakiyama, T., Matsuda, H., Morita, C., Natural vibration study on rectangular plates with a line hinge and various boundary conditions, *Journal of Sound and Vibration*, 322:227-240, 2009.

Jones, R. M., *Mechanics of Composite Materials*, Taylor and Francis, 1999.

Kantorovich, L., Krylov, V., *Approximate Methods of Higher Analysis*. Interscience Publishers, 1964.

Leitmann, G., *The Calculus of Variations and Optimal Control*, Plenum Press, 1986.

Lekhnitskii , S.G., *Anisotropic Plates*, Gordon and Breach Science Publishers, 1968.

Mikhlin S., *Variational Methods of Mathematical Physics*, Mac Millan, 1964.

Quintana, M. V., and Grossi, R. O., Free vibrations of a generally restrained rectangular plate with an internal line hinge, *Applied Acoustics*, 73(4): 356-365, 2012.

Reddy, J. N., *Mechanics of Laminated Anisotropic Plates: Theory and Analysis*, CRC Press, 1997.

Sagan H., *Introduction to the Calculus of Variations*, Mc Graw Hill Book Co., 1969.

Szilard, R., *Theory and Analysis of Plates*, Prentice Hall, 1974.

Timoshenko, S., Krieger, W., *Theory of Plates and Shells,* Mc Graw Hill, 1959.

Troutman, J. L., *Variational Calculus and Optimal Control*, Springer-Verlag, 1996.

Wang, C. M., Xiang, Y., C., Wang, Y., Buckling and vibration of plates with an internal line hinge via the Ritz method, *Proceedings of First Asian-Pacific Congress on Computational Mechanics, Sydney*, 1663-1672, 2001.

Weinstock, R., *Calculus of Variations with Applications to Physics and Engineering*, Dover Publications, 1974.

Whitney, J. M., *Structural Analysis of Laminated Anisotropic Plates*, Technomic Publishing Co. Inc., 1987.

Xiang, Y., and Reddy, J. N., Natural vibration of rectangular plates with an internal line hinge using the first order shear deformation plate theory, *Journal of Sound and Vibration*, 263:285-297, 2003.